D. Aristizabal Sierra, A. VicentePRD

KIAS-P15060

# $h, Z \to \ell_i \bar{\ell}_j$, $\Delta a_\mu$, $\tau \to (3\mu, \mu\gamma)$ in generic two-Higgs-doublet models


R. Benbrik *,[1,2] Chuan-Hung Chen †,[3] and Takaaki Nomura ‡[4]

[1] *LPHEA, Semlalia, Cadi Ayyad University, Marrakech, Morocco*

[2] *MSISM Team, Faculté Polydisciplinaire de Safi, Sidi Bouzid B.P 4162, 46000 Safi, Morocco*

[3] *Department of Physics, National Cheng-Kung University, Tainan 70101, Taiwan*

[4] *School of Physics, Korea Institute for Advanced Study, Seoul 130-722, Republic of Korea*



(Dated: November 30, 2015)



## Abstract

Inspired by a significance of $2.4\sigma$ in $h \to \mu\tau$ decay observed by CMS at $\sqrt{s} = 8$ TeV, we investigate the Higgs lepton flavor violating effects in the generic two-Higgs-doublet model (GTHDM), where the lepton flavor changing neutral currents are induced at tree level and arisen from Yukawa sector. We revisit the constraints for GTHDM by considering theoretical requirements, precision measurements of $\delta\rho$ and oblique parameters $S$, $T$, $U$ and Higgs measurements. The bounds from Higgs data now play the major role. With the values of parameters that simultaneously satisfy the Higgs bounds and the excess of Higgs coupling to $\mu$-$\tau$ at CMS, we find that the tree-level $\tau \to 3\mu$ and loop-induced $\tau \to \mu\gamma$ could be consistent with current experimental upper limits; the discrepancy in muon $g-2$ between experiment and standard model prediction could be solved; and an interesting relation between muon $g-2$ and branching ratio (BR) for $\mu \to e\gamma$ is found. The GTHM results that the ratio $BR(h \to e\tau)/BR(h \to \mu\tau)$ should be smaller than $10^{-4}$ in order of magnitude. Additionally, we also study the rare decay $Z \to \mu\tau$ and get $BR(Z \to \mu\tau) < 10^{-6}$.





* Email: rbenbrik@ictp.it

† Email: physchen@mail.ncku.edu.tw

‡ Email: nomura@kias.re.kr

The observed flavor changing neutral currents (FCNCs) in the standard model (SM) occur at loop level of quark sector and they are originated from $W$-mediated charged currents, such as $K-\bar{K}$, $B-\bar{B}$ and $D-\bar{D}$ mixings, $b \to s\gamma$, etc. Due to the loop effects, it is believed that these FCNC processes are sensitive to the new physics. However, most of these processes involve large uncertain nonperturbative QCD effects, therefore, even there exist new physics, it is not easy to distinguish them from the SM results due to the QCD uncertainty.

The situation in lepton sector is different. Although the SM also has lepton FCNCs, e.g. $\mu \to e\gamma, \tau \to (e,\mu)\gamma$, however they are irrelevant to QCD effects and highly suppressed; if any signal is observed, definitely that is a strong evidence for the new physics. Therefore, it becomes an important issue to search for new physics through lepton sector [1].

By the discovery of a new scalar with a mass of around 125 GeV at ATLAS [2] and CMS-[3], we have taken one step further in understanding the electroweak symmetry breaking (EWSB) through spontaneous symmetry breaking (SSB) mechanism in the scalar sector. With $\sqrt{s} = 13-14$ TeV, the next step for the high luminosity LHC is to explore not only the detailed properties of the observed scalar but also the existence of other Higgs scalars and new physics effects.

CMS [4] and ATLAS [5] recently report the measurements of $h \to \mu\tau$ decay in $pp$ collisions at $\sqrt{s} = 8$ TeV successively. At 95% confidence level (CL), the branching ratio (BR) for the decay at CMS is $BR(h \to \mu\tau) < 1.51\%$ while ATLAS gives $BR(h \to \mu\tau) < 1.85\%$ . Additionally, a slight excess of events with a significance of $2.4\sigma$ is reported by CMS and the best fit is $BR(h \to \mu\tau) = (0.84^{+0.39}_{-0.37})\%$. If the excess is not a statistical issue, the extension of the SM becomes necessary. Inspired by the excess of events, the possible new physics effects are studied by the authors in Refs. [6–26]. The earlier works could also refer to Refs. [27–34].

Following the measurements of ATLAS and CMS on the couplings of Higgs to leptons, we are going to investigate the lepton flavor violation (LFV) in the generic two-Higgs-doublet model (THDM) [35]. In the THDM, there are five physical scalar particles and they are: two CP-even bosons, one CP-odd pseudoscalar and one charged Higgs boson. According to the fashion that Higgs doublets couple to fermions, the THDM is classified as type-I, -II, -III, lepton specific model and flipped model [36]. The minimal supersymmetric SM (MSSM) belongs to the type-II THDM, in which one Higgs doublet couples to up-type quarks while the other couples to down-type quarks. The type-III THDM corresponds to the case that each of both Higgs doublets could couple to all fermions simultaneously. As a result, the tree level FCNCs in the quark and charged lepton sectors are induced. When the strict experimental data are taken into account, it is interesting to see and understand the impacts of type-III model on the LFV.

If we assume no new CP violating source from the scalar sector, like type-II model and MSSM, the main new free parameters are masses of new scalars, $\tan\beta = v_2/v_1$ and angle $\alpha$, where the $\tan\beta$ is related to the ratio of vacuum expectation values (VEVs) of two Higgs fields and the angle $\alpha$ stands for the mixing effect of two CP-even scalars. Basically these two parameters have been constrained strictly by current experimental data, such as $\rho$-parameter, $S$, $T$ and $U$ oblique parameters, Higgs searches through $h \to (\gamma\gamma, WW^*, ZZ^*, \tau\tau, b\bar{b})$, etc. In order to show the correlation of free parameters on these experimental bounds, we revisit the constraints by adopting the $\chi$-square fitting approach. We will see that although the allowed value of $\cos(\beta-\alpha)$ is approaching to the decoupling limit, i.e. $\alpha \sim \beta - \pi/2$, if $\cos\beta$ is small enough, the BR for $h \to \mu\tau$ could still be as large as the measurements of ATLAS and CMS.

Besides $h \to \ell_i \bar{\ell}_j$ decays, the type-III model also has significant effects on other lepton flavor conserving and violating processes, such as muon anomalous magnetic moment, $\mu \to 3e$, $\mu(\tau) \to e(\mu, e)\gamma$, $Z \to \ell_i \bar{\ell}_j$, etc. Although we have not observed concrete signals for lepton flavor violating processes, however, the current experimental data have put strict limits on $\mu \to 3e$ and $\mu \to e\gamma$ with $BR(\mu \to 3e) < 10^{-12}$ and $BR(\mu \to e\gamma) < 5.7 \times 10^{-13}$ [37]. Combing the LHC data and upper limits from rare lepton decays, we study if the excess of muon $g-2$ can be solved and the BRs of the listed lepton FCNC processes could be significant in the type-III THDM.

For displaying the scalar couplings to fermions in type-III model, we start writing the Yukawa sector to be

$$\begin{aligned} -\mathcal{L}_Y &= \bar{Q}_L Y_1^u U_R \tilde{H}_1 + \bar{Q}_L Y_2^u U_R \tilde{H}_2 \\ &+ \bar{Q}_L Y_1^d D_R H_1 + \bar{Q}_L Y_2^d D_R H_2 \\ &+ \bar{L} Y_1^\ell \ell_R H_1 + \bar{L} Y_2^\ell \ell_R H_2 + h.c.\,, \end{aligned} \tag{1}$$

where we have hidden all flavor indices, $Q_L^T = (u, d)_L$ and $L^T = (\nu, \ell)_L$ are the $SU(2)_L$ quark and lepton doublets, $Y_{1,2}^f$ are the Yukawa matrices, $\tilde{H}_i = i\tau_2 H_i^*$ with $\tau_2$ being the second

Pauli matrix, the Higgs doublets are represented by

$$H_i = \begin{pmatrix} \phi_i^+ \\ (v_i + \phi_i + i\eta_i)/\sqrt{2} \end{pmatrix} \tag{2}$$

and $v_i$ is VEV of $H_i$. Eq. (1) could recover the type-II THDM if $Y_1^u$, $Y_2^d$ and $Y_2^\ell$ vanish. Before EWSB, all $Y_{1,2}^f$ are arbitrary $3\times 3$ matrices and fermions are not physical eigenstates; therefore, we have the freedom to choose $Y_1^u$, $Y_2^d$ and $Y_2^\ell$ to be diagonal forms, that is, $Y_1^u = \mathrm{diag}(y_1^u, y_2^u, y_3^u)$ and $Y_2^{d,\ell} = \mathrm{diag}(y_1^{d,\ell}, y_2^{d,\ell}, y_3^{d\ell})$.

The VEVs $v_{1,2}$ are dictated by the scalar potential, where the gauge invariant form is given by [36]

$$\begin{aligned} V(\Phi_1,\Phi_2) &= m_1^2\Phi_1^\dagger\Phi_1 + m_2^2\Phi_2^\dagger\Phi_2 - (m_{12}^2\Phi_1^\dagger\Phi_2 + \mathrm{h.c}) + \frac{1}{2}\lambda_1(\Phi_1^\dagger\Phi_1)^2 \\ &+ \frac{1}{2}\lambda_2(\Phi_2^\dagger\Phi_2)^2 + \lambda_3(\Phi_1^\dagger\Phi_1)(\Phi_2^\dagger\Phi_2) + \lambda_4(\Phi_1^\dagger\Phi_2)(\Phi_1^\dagger\Phi_2) \\ &+ \left[\frac{\lambda_5}{2}(\Phi_1^\dagger\Phi_2)^2 + \left(\lambda_6\Phi_1^\dagger\Phi_1 + \lambda_7\Phi_2^\dagger\Phi_2\right)\Phi_1^\dagger\Phi_2 + \mathrm{h.c.}\right], \end{aligned} \tag{3}$$

Since we do not concentrate on the CP violating issue, we set the parameters in Eq. (3) be real numbers. In addition, we also require the CP phase arisen from ground state to vanish [35]. By the scalar potential with CP invariance, we have 10 free parameters. In our approach, the eight of ten parameters are taken as

$$\{m_h\,, m_H\,, m_A\,, m_{H^\pm}\,, m_{12}^2\,, v\,, \tan\beta\,, \alpha\} \tag{4}$$

with $v = \sqrt{v_1^2 + v_2^2}$. Without loss of the generality, in phenomenological analysis, we set $\lambda_{6,7} \ll 1$. The physical states for scalars are expressed by

$$\begin{aligned} h &= -s_\alpha\phi_1 + c_\alpha\phi_2\,, \\ H &= c_\alpha\phi_1 + s_\alpha\phi_2\,, \\ H^\pm(A) &= -s_\beta\phi_1^\pm(\eta_1) + c_\beta\phi_2^\pm(\eta_2) \end{aligned} \tag{5}$$

with $c_\alpha(s_\alpha) = \cos\alpha(\sin\alpha)$, $c_\beta = \cos\beta = v_1/v$, $s_\beta = \sin\beta = v_2/v$. In this study, $h$ is the SM-like Higgs while $H$, $A$ and $H^\pm$ are new stuff in the THDM.

Using Eqs. (1) and (2), one can easily find that the mass matrix for fermion is

$$\mathbf{M}_f = \frac{v}{\sqrt{2}}\left(\cos\beta Y_1^f + \sin\beta Y_2^f\right). \tag{6}$$

If we introduce the unitary matrices $V_L^f$ and $V_R^f$, the mass matrix can be diagonalized through $\mathbf{m}_f = V_L^f \mathbf{M}_f V_R^{f\dagger}$. Accordingly, the scalar couplings to fermions could be formulated by

$$-\mathcal{L}_{Y\phi} = \bar{\ell}_L \, \epsilon_\phi \mathbf{y}_\phi^\ell \, \ell_R \, \phi + \bar{\nu}_L V_{\rm PMNS} \, \mathbf{y}_{H^\pm}^\ell \, \ell_R \, H^+ + h.c. \, , \tag{7}$$

where $\phi = h, H, A$ stands for the possible neutral scalar boson, $\epsilon_{h(H)} = 1$, $\epsilon_A = i$,$V_{\rm PMNS}$ is the Pontecorvo-Maki-Nakagawa-Sakata matrix and the Yukawa couplings $\mathbf{y}_{\phi,H^\pm}^\ell$ are defined by

$$\boxed{\begin{aligned}
(\mathbf{y}_h^\ell)_{ij} &= -\frac{s_\alpha}{c_\beta}\frac{m_i}{v}\delta_{ij} + \frac{c_{\beta\alpha}}{c_\beta} X_{ij}^\ell \, , \\
(\mathbf{y}_H^\ell)_{ij} &= \frac{c_\alpha}{c_\beta}\frac{m_i}{v}\delta_{ij} - \frac{s_{\beta\alpha}}{c_\beta} X_{ij}^\ell \, , \\
(\mathbf{y}_A^\ell)_{ij} &= -\tan\beta \frac{m_i}{v}\delta_{ij} + \frac{X_{ij}^\ell}{c_\beta} \, ,
\end{aligned}} \tag{8}$$

Note: Non-diagonal terms vanishfor c

and $\mathbf{y}_{H^\pm}^\ell = \sqrt{2}\mathbf{y}_A^\ell$ with $c_{\beta\alpha} = \cos(\beta - \alpha)$, $s_{\beta\alpha} = \sin(\beta - \alpha)$ and

$$\mathbf{X^u} = V_L^u \frac{Y_1^u}{\sqrt{2}} V_R^{u\dagger} \, , \ \mathbf{X^d} = V_L^d \frac{Y_2^d}{\sqrt{2}} V_R^{d\dagger} \, \ \boxed{\mathbf{X}^\ell = V_L^\ell \frac{Y_2^\ell}{\sqrt{2}} V_R^{\ell\dagger} \, .} \tag{9}$$

By the formulation, one can see that the Yukawa couplings of Higgses to fermions could return to type-II THDM when $Y_1^u$ and $Y_2^{d,\ell}$ vanish. On the other hand, the FCNC effects are also associated with $Y_1^u$ and $Y_2^{d,\ell}$, which could be chosen to be diagonal matrices as mentioned earlier. The detailed Yukawa couplings of $H$, $A$ and $H^\pm$ to up- and down-type quarks are summarized in Appendix.

In principle, $Y_{1,2}^f$ are arbitrary free parameters. In order to get more connections among parameters and reduce the number of free parameters, hermitian Yukawa matrices can achieve the intention, where the hermiticity of Yukawa matrix can be realized by symmetry, such as the global (gauged) horizontal $SU(3)_H$ symmetry [40], left-right symmetry [41], etc. Therefore, the equality $V_L^f = V_R^f \equiv V^f$ can be satisfied naturally. With the diagonal $Y_1^u$ and $Y_2^{d,\ell}$, the $Xs'$ effects in Eq. (9) can be expressed by $X_{ij}^f = V_{ik}^f V_{jk}^{f*} y_k^f$ with a sum in $k$. Since no CP violation is observed in lepton sector, it is plausible to assume $Y_{1,2}^\ell$ to be real numbers. Following this assumption, we get that $\mathbf{X}^\ell$ is a symmetric matrix, i.e. $X_{ij}^\ell = X_{ji}^\ell$. In the decoupling limit of $\alpha = \beta - \pi/2$, the Yukawa couplings in Eq. (8) become

$$\begin{aligned}
(\mathbf{y}_h^\ell)_{ij} &= \frac{m_i}{v}\delta_{ij} \, , \\
(\mathbf{y}_H^\ell)_{ij} &= -(\mathbf{y}_A^\ell)_{ij} = \tan\beta \frac{m_i}{v}\delta_{ij} - \frac{1}{c_\beta} X_{ij}^\ell \, .
\end{aligned} \tag{10}$$

In such limit, we see that the tree-level lepton FCNCs are suppressed in $h$ decays, however they are still allowed in $H$ and $A$ decays.

Next, we discuss the scalar-mediated lepton flavor violating effects on the interesting processes. Using the couplings in Eq. (7), the BR for $h \to \tau\mu$ is given by

$$BR(h \to \mu\tau) = \frac{c_{\beta\alpha}^2(|X_{23}^\ell|^2 + |X_{32}^\ell|^2)}{16\pi c_\beta^2 \Gamma_h} m_h . \tag{11}$$

With $m_h = 125$ GeV, $\Gamma_h \approx 4.21$ MeV and $X_{32}^\ell = X_{23}^\ell$, we can get the information of $X_{23}^\ell$ as

$$X_{23}^\ell = 3.77 \times 10^{-3} \left(\frac{c_\beta}{0.02}\right)\left(\frac{0.01}{c_{\beta\alpha}}\right)\sqrt{\frac{BR(h\to\mu\tau)}{0.84\times 10^{-2}}} , \tag{12}$$

where $BR(h \to \mu\tau)$ could be taken from the experimental data. If one adopts the ansatz $X_{\mu\tau}^\ell = \sqrt{m_\mu m_\tau}/v\chi_{\mu\tau}^\ell$, $\chi_{\mu\tau}^\ell \sim 2$ could fit the current CMS excess.

Moreover, we find that the same $X_{23}^\ell$ effects can also induce the decay $\tau \to 3\mu$ at tree level through the mediation of scalar bosons and the BR could be formulated by

$$BR(\tau \to 3\mu) = \frac{\tau_\tau m_\tau^5}{3\cdot 2^9 \pi^3}\frac{|X_{23}^\ell|^2}{c_\beta^2}\left[\left|\frac{c_{\beta\alpha}y_{h22}^\ell}{m_h^2} - \frac{s_{\beta\alpha}y_{H22}^\ell}{m_H^2}\right|^2 + \left|\frac{y_{A22}^\ell}{m_A^2}\right|^2\right] \tag{13}$$

with $\tau_\tau$ being the lifetime of tauon. Eq. (13) could be applied to $\mu \to 3e$ when the corresponding quantities are correctly replaced. If we set $X_{ij}^\ell = \sqrt{m_i m_j}/v\chi_{ij}^\ell$ and assume that $\chi_{ij}^\ell = \chi^\ell$ are independent of lepton flavors, the ratio of $BR(\mu \to 3e)$ to $BR(\tau \to 3\mu)$ could be naively estimated as

$$R_{\mu/\tau} \sim \frac{\tau_\mu}{\tau_\tau}\frac{m_\mu^5}{m_\tau^5}\frac{m_e^3}{m_\tau m_\mu^2} = 3.5\times 10^{-8} . \tag{14}$$

With the current upper limit $BR(\tau \to 3\mu) < 2.1 \times 10^{-8}$ [37], we see $BR(\mu \to 3e) < 7.5 \times 10^{-16}$ in type-III model, which is far smaller than the current upper bound. Nevertheless, the suppression factor of $m_e^3/(m_\tau m_\mu^2)$ in Eq. (14) could be relaxed to be $m_e/m_\tau$ at one-loop level, where the lepton-pair is produced by virtual $\gamma/Z$ in the SM. Since the $X_{23}^\ell$ parameter will also appear in $\mu \to e\gamma$ and $\tau \to \mu\gamma$, which have stronger limits in experiments, therefore, in following analysis we don't further discuss these processes. Additionally, for removing the correlation between $\tau \to 3\mu$ and $\mu \to 3e$, $\chi_{ij}^\ell$ could be taken as flavor dependence.

It has been known that the discrepancy in muon $g-2$ between experimental data and SM prediction now is $\Delta a_\mu = a_\mu^{\rm exp} - a_\mu^{\rm SM} = (28.8 \pm 8.0) \times 10^{-10}$ [37]. Although muon $g-2$ is a flavor conserving process, $X_{23}^\ell$ and $X_{21}^\ell$ also contribute to the anomaly through the loops mediated by the neutral and charged Higgses. Thus, the muon anomaly in type-III model can be formulated by [38, 55]

$$\begin{aligned}\Delta a_\mu &\simeq \frac{m_\mu m_\tau X^\ell_{23} X^\ell_{32}}{8\pi^2 c^2_\beta} Z_\phi \,, \qquad (15)\\ Z_\phi &= \frac{c^2_{\beta\alpha}\left(\ln(m^2_h/m^2_\tau) - \frac{3}{2}\right)}{m^2_h} + \frac{s^2_{\beta\alpha}\left(\ln(m^2_H/m^2_\tau) - \frac{3}{2}\right)}{m^2_H}\\ &- \frac{\ln(m^2_A/m^2_\tau) - \frac{3}{2}}{m^2_A}\,,\end{aligned}$$

where we have dropped the subleading terms associated with $m^2_\mu$. We will explore the question: when the current strict experimental data are considered, could the anomaly of $\Delta a_\mu$ be explained in type-III model?

As mentioned earlier, the radiative lepton decays $\mu \to e\gamma$ and $\tau \to (\mu, e)\gamma$ in the SM are very tiny and sensitive to new physics effects. In type-III model, these radiative decays could be generated by charged and neutral Higgses through the FCNC effects. For illustration, we present the effective interaction for $\mu \to e\gamma$ as

$$\mathcal{L}_{\mu\to e\gamma} = \frac{e m_\mu}{16\pi^2} \bar{e}\sigma_{\mu\nu}\left(C_L P_L + C_R P_R\right)\mu F^{\mu\nu}\,, \qquad (16)$$

where $F^{\mu\nu}$ is the electromagnetic field strength tensor, the Wilson coefficients $C_L$ and $C_R$ from neutral and charged scalars are given by

$$\begin{aligned}C_{L(R)} &= C^\phi_{L(R)} + C^{H^\pm}_{L(R)}\,,\\ C^\phi_L &= \frac{X^\ell_{32} X^\ell_{13}}{2c^2_\beta}\frac{m_\tau}{m_\mu} Z_\phi\,,\\ C^{H^\pm}_L &= -\frac{1}{12 m^2_{H^\pm}}\left(\frac{2X^\ell_{23} X^\ell_{13}}{c^2_\beta}\right)\,, \qquad (17)\end{aligned}$$

$C^\phi_R = C^\phi_L$, $C^{H^\pm}_R = 0$, and the BR for $\mu \to e\gamma$ is

$$\frac{BR(\mu\to e\gamma)}{BR(\mu \to e\bar{\nu}_e\nu_\mu)} = \frac{3\alpha_e}{4\pi G^2_F}\left(|C_L|^2 + |C_R|^2\right)\,. \qquad (18)$$

We see that the factor $Z_\phi$ in $\Delta a_\mu$ also appears in $C^\phi_{L(R)}$. In terms of $\Delta a_\mu$ in Eq. (15), $C^\phi_{L(R)}$ can be expressed as

$$C^\phi_{L(R)} = \frac{X^\ell_{13}}{X^\ell_{23}}\frac{4\pi^2\Delta a_\mu}{m^2_\mu}\,. \qquad (19)$$

Since $C^{\phi}_{L(R)}$ has an enhanced factor $m_\tau/m_\mu$, the contribution from charged Higgs becomes the subleading effect. The formulas for $\tau \to \mu\gamma$ could be found in Appendix. From Eq. (17), we see that if flavor changing effects $X^{\ell}_{ij} = 0$ with $i \neq j$, the effective Wilson coefficients $C_{L,R}$ vanish. That is, the contributions to the radiative lepton decays from other types of THDM are suppressed. Therefore, if any sizeable signals of $\mu \to e\gamma$ and $\tau \to \mu\gamma$ are observed, that will be a strong support for type-III model.

The last process that we are interested in is the decay $Z \to \mu\tau$. Other flavor changing leptonic $Z$ decays also occur in type-III model, however, since $\mu\tau$ mode is the dominant one; therefore, in current study we just focus on the $\mu\tau$ channel. Besides the $Z$ coupling to charged leptons, in the THDM, $Z$-$h(H)$-$A$ and $Z$-$Z$-$h(H)$ interactions are also involved, in which the vertices are [42]

$$
\begin{aligned}
Z - h(H) - A: &\quad -\frac{g c_{\beta\alpha}(-s_{\beta\alpha})}{2\cos\theta_W}(p_A + p_{h(H)})_\mu \,, \\
Z - H^+ - H^-: &\quad -i\frac{g\cos 2\theta_W}{2\cos\theta_W}(p_{H^+} + p_{H^-})_\mu \,, \\
Z - Z - h(H): &\quad \frac{g m_Z}{\cos\theta_W} s_{\beta\alpha}(c_{\beta\alpha}) g_{\mu\nu}
\end{aligned} \tag{20}
$$

with $\theta_W$ being the Weinberg's angle. The typical Feynman diagrams for $Z \to \mu\tau$ are presented in Fig. 1. Since there involve lots of one-loop Feynman diagrams in the process,

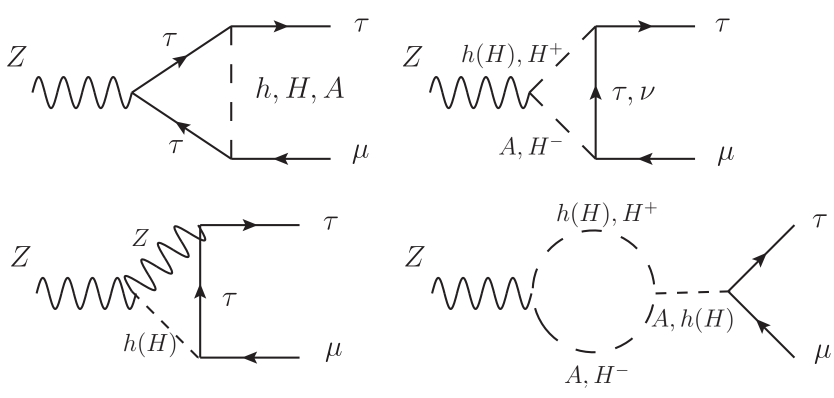


FIG. 1: Representative Feynman diagrams for $Z \to \mu\tau$ decay.

we employ the FormCalc package [43] to deal with the loop calculations. We do not show the lengthy formulas in the paper, instead we directly display the numerical results.

Before presenting the numerical analysis, we discuss the theoretical and experimental constraints. The main theoretical constraints of THDM are the perturbative scalar potential, vacuum stability and unitarity. Therefore, in order to satisfy perturbative requirement, we set that all quartic couplings of the scalar potential obey $|\lambda_i| \leq 8\pi$ for all $i$. The conditions for vacuum stability are [45, 46]

$$\begin{aligned}
&\lambda_1 > 0\,, \qquad \lambda_2 > 0\,, \lambda_3 + \sqrt{\lambda_1 \lambda_2} > 0, \quad \sqrt{\lambda_1 \lambda_2} + \lambda_3 + \lambda_4 - |\lambda_5| > 0, \\
&2|\lambda_6 + \lambda_7| \leq \frac{1}{2}(\lambda_1 + \lambda_2) + \lambda_3 + \lambda_4 + \lambda_5\,.
\end{aligned} \tag{21}$$

Without losing the general properties, we set $\lambda_{6,7} \ll 1$ in our numerical analysis. Effectively, the scalar potential is similar to the type-II THDM. Since the unitarity constraint involves a variety of scattering processes, here we adopt the results in Ref. [44].

Next, we briefly state the experimental bounds. It is known that $b \to s\gamma$ is sensitive to the mass of charged Higgs. According to the recent analysis in Ref. [50], the lower bound in type-II model is given to be $m_{H^\pm} > 480$ GeV at 95% CL. Due to the neutral and charged Higgses involved in the self-energy of W and Z bosons, the precision measurements of $\rho$-parameter and the oblique parameters, denoted by S, T and U [47], could give constraints on the associated new parameters. By the global fit, we know $\rho = 1.00040 \pm 0.00024$ [37] and the SM prediction is $\rho = 1$. Taking $m_h = 125$ GeV, $m_t = 173.3$ GeV and assuming $U = 0$, the tolerated ranges for S and T are found by [48]

$$\Delta S = 0.06 \pm 0.09\,, \quad \Delta T = 0.10 \pm 0.07\,, \tag{22}$$

where the correlation factor is $\rho = +0.91$, $\Delta S = S^{\rm 2HDM} - S^{\rm SM}$, $\Delta T = T^{\rm 2HDM} - T^{\rm SM}$, and their explicit expressions can be found in Ref. [49]. We note that in the limit $m_{H^\pm} = m_{A^0}$, $\Delta T$ vanishes.

Since the Higgs data are approaching precision measurement, the relevant measurements now could give strict limits on $c_{\beta\alpha}$ and $s_\alpha$. As usual, the Higgs measurement is expressed by the signal strength, which is defined by the ratio of Higgs signal to the SM prediction and given by

$$\mu_i^f = \frac{\sigma_i(h) \cdot BR(h \to f)}{\sigma_i^{SM}(h) \cdot BR^{SM}(h \to f)} \equiv \bar{\sigma}_i \cdot \mu_f\,. \tag{23}$$

$\sigma_i(h)$ denotes the Higgs production cross section by channel $i$ and $BR(h \to f)$ is the BR for the Higgs decay $h \to f$. Since several Higgs boson production channels are available at the LHC, we are interested in the gluon fusion production ($ggF$), $t\bar{t}h$, vector boson fusion (VBF) and Higgs-strahlung $Vh$ with $V = W/Z$; and we group them to be $\mu^f_{ggF+t\bar{t}h}$ and

$\mu^f_{VBF+Vh}$. The values of observed signal strengths are shown in Table. I, where we have used the notations $\widehat{\mu}^f_{ggF+t\bar{t}h}$ and $\widehat{\mu}^f_{VBF+Vh}$ to express the combined results of ATLAS [51] and CMS [52].

TABLE I: Combined best-fit signal strengths $\widehat{\mu}_{\rm ggF+tth}$ and $\widehat{\mu}_{\rm VBF+Vh}$ and the associated correlation coefficient $\rho$ for the corresponding Higgs decay mode [51, 52].

| $f$ | $\widehat{\mu}^f_{\rm ggF+tth}$ | $\widehat{\mu}^f_{\rm VBF+Vh}$ | $\pm\, 1\widehat{\sigma}_{\rm ggF+tth}$ | $\pm\, 1\widehat{\sigma}_{\rm VBF+Vh}$ | $\rho$ |
|---|---|---|---|---|---|
| $\gamma\gamma$ | 1.32 | 0.8 | 0.38 | 0.7 | -0.30 |
| $ZZ^*$ | 1.70 | 0.3 | 0.4 | 1.20 | -0.59 |
| $WW^*$ | 0.98 | 1.28 | 0.28 | 0.55 | -0.20 |
| $\tau\tau$ | 2 | 1.24 | 1.50 | 0.59 | -0.42 |
| $b\bar{b}$ | 1.11 | 0.92 | 0.65 | 0.38 | 0 |

In order to study the influence of new free parameters and to understand their correlations, we employ the minimum $\chi$-square method when the experimental data are considered. For a given Higgs decay channel $f = \gamma\gamma, WW^*, ZZ^*, \tau\tau$, we define the $\chi^2_f$ as

$$\chi^2_f = \frac{1}{\hat{\sigma}^2_1(1-\rho^2)}(\mu^f_1 - \hat{\mu}^f_1)^2 + \frac{1}{\hat{\sigma}^2_1(1-\rho^2)}(\mu^f_2 - \hat{\mu}^f_2)^2 - \frac{2\rho}{\hat{\sigma}_1\hat{\sigma}_2(1-\rho^2)}(\mu^f_1 - \hat{\mu}^f_1)(\mu^f_2 - \hat{\mu}^f_2)\,, \quad (24)$$

where $\hat{\mu}^f_{1(2)}$, $\hat{\sigma}_{1(2)}$ and $\rho$ are the measured Higgs signal strength, the one-sigma errors, and the correlation, respectively, the corresponding values could refer to Table I, the indices 1 and 2 in turn stand for $\rm ggF + tth$ and $\rm VBF + Vh$, and $\mu^f_{1,2}$ are the results in the 2HDM. The global $\chi$-square is defined by

$$\chi^2 = \sum_f \chi^2_f + \chi^2_{ST}\,, \quad (25)$$

where $\chi^2_{ST}$ is the $\chi^2$ for S and T parameters, its definition can be obtained from Eq.(24) by using the replacements $\mu^f_1 \to S^{\rm 2HDM}$ and $\mu^f_2 \to T^{\rm 2HDM}$, and the corresponding values can be found from Eq. (22).

Besides the bounds from theoretical considerations, Higgs data and upper limit $BR(\mu \to 3e) < 1.0 \times 10^{-12}$, the schemes for the setting of parameters in the study are adopted as follows: the masses of SM Higgs and charged Higgs are fixed to be $m_h = 125.5$ GeV and

$m_{H^\pm} = 500$ GeV and the regions of other involving parameters are chosen as

$$m_{H,A} \supset [126, 1000]\,\text{GeV}\,, \quad m_{12}^2 \supset [-1.0, 1.5] \times 10^5\,\text{GeV}^2\,,$$
$$\tan\beta \supset [0.5, 50]\,, \quad \alpha = [-\pi/2, \pi/2]\,. \tag{26}$$

Since our purpose is to show the impacts of THDM on LFV, for lowering the influence of quark sector, we set $\mathbf{X}^q \sim 0$ in current analysis, i.e. Yukawa couplings of quarks behave like a type-II THDM. The influence of $X^q \neq 0$ could be found in Ref. [53]. For understanding the small FCNCs at lepton sector, we use the ansatz $X^\ell_{ij} = \sqrt{m_i m_j}/v \chi^\ell_{ij}$; thus, $\chi^\ell_{ij}$ could be of order of one. Although $h$-$\ell^+$-$\ell^-$ couplings also contribute to $h \to 2\gamma$ process, unless one makes an extreme tuning on $\chi^\ell_{ii}$, otherwise, their contributions to $h \to 2\gamma$ are small in THDM.

We now start investigating the numerical analysis. Combining the theoretical requirements and $\delta\rho = (4.0 \pm 2.4) \times 10^{-4}$, the allowed ranges of $\tan\beta$ and $c_{\beta\alpha}$ are shown by yellow dots in Fig. 2 , where the scanned regions of Eq. (26) have been used. When the measurements of oblique parameters are included, the allowed parameter space is changed slightly and shown by blue dots in Fig. 2. In both cases, data with $2\sigma$ errors are adopted. By the results, we see that the constraint on $c_{\beta\alpha}$ is loose and the favorable range for $\tan\beta$ is $\tan\beta < 20$.

To perform the constraints from Higgs data listed in Table I, we use minimum $\chi$-square approach. The best fit is taken at 68%, 95.5% and 99.7% CL, that is, the corresponding errors of $\chi^2$ are $\Delta\chi^2 \leq 2.3$, 5.99 and 11.8, respectively. With the definitions in Eqs. (24) and (25), we present the allowed values of parameters in Fig. 3(a), where the theoretical requirements, $\delta\rho$, oblique parameters and Higgs data are all included and the colors in the plots stand for 68% (blue), 95.5% (green) and 99.7% (red) CL. It is clear that $c_{\beta\alpha}$ has been limited to a narrow range and the favorable values of $\tan\beta$ are less than 10. We can understand the correlation between angle $\beta$ and $\alpha$ in Fig. 3(b). We will use the results to study other rare decays. For calculating $\Delta a_\mu$ and rare tau, $\mu$ and $Z$ decays, we need the information about the allowed masses of $H$ and $A$. Using the results of $\chi$-square fit, we present the correlation between $m_H - m_{H^\pm}$ and $m_A - m_H$ in Fig. 4(a) and the correlation between $m_{12}^2$ and $m_A - m_H$ in Fig. 4(b), where the ranges of parameters in Eq. (26) have been satisfied.

After obtaining the allowed ranges of parameters, we now analyze the implications of

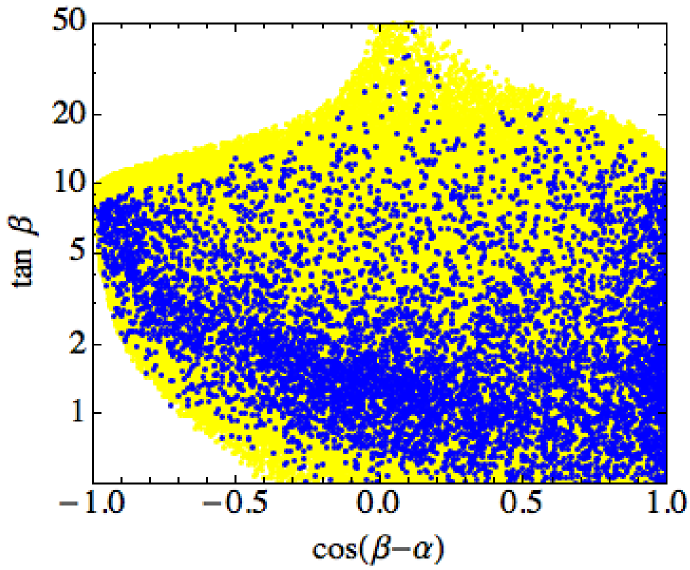


FIG. 2: Constraints from theoretical requirements and precision measurement of $\rho$-parameter are shown by yellow dots; and the results including the measurements of oblique parameters are displayed by blue dots.

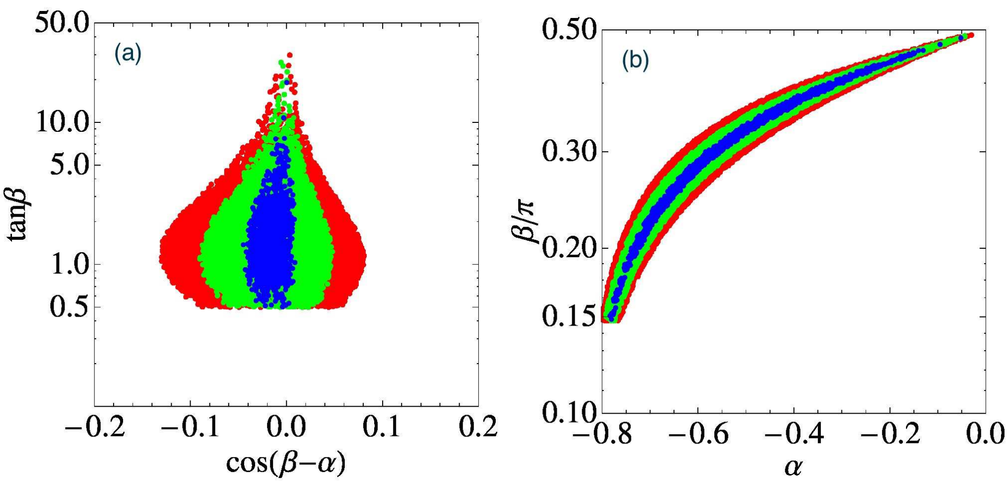


FIG. 3: Bounds with $\chi$-square fit as a function of (a) $\tan\beta$ and $\cos(\beta-\alpha)$ and (b) $\beta/\pi$ and $\alpha$, where the blue, green and red denote the $\Delta\chi^2 \leq 2.3$, 5.99 and 11.8, respectively.

lepton flavor violating effects on $h \to \mu\tau$ and other rare decays. By Eq. (11), we see that $h \to \mu\tau$ decay is sensitive to $c_{\beta\alpha}$, $\tan\beta$ and $\chi^{\ell}_{23}$. In order to understand under what condition the CMS result of $h \to \mu\tau$ can be reached in type-III THDM, we show the contour for $BR(h \to \mu\tau) = 0.84\%$ as a function of $\tan\beta$ and $c_{\beta\alpha}$ in Fig. 5(a), where the solid and dashed lines stand for $\chi^{\ell}_{23} = 4$ and 6, respectively. We find that in order to fit the central

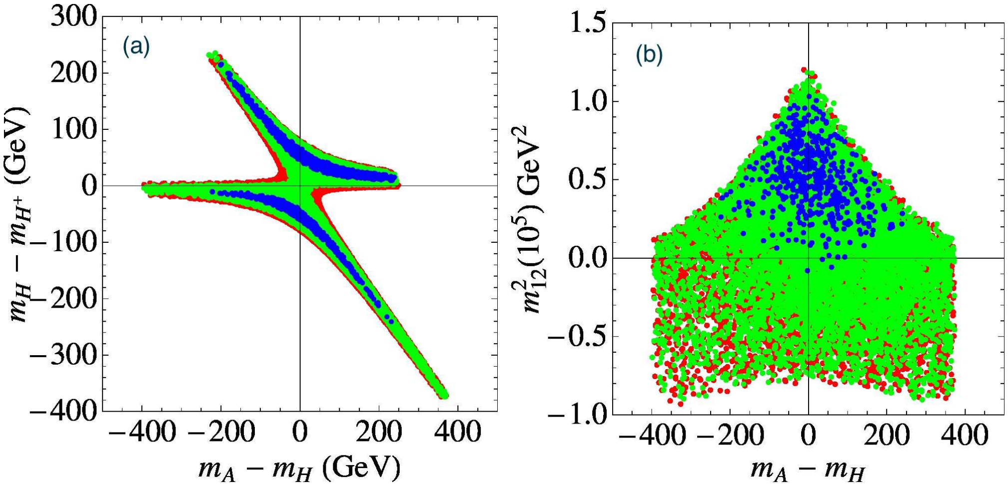


FIG. 4: Correlation between (a) $m_H - m_{H^\pm}$ and $m_A - m_H$ and (b) $m_{12}^2$ and $m_A - m_H$, where the blue, green and red denote the $\Delta\chi^2 \leq 2.3$, 5.99 and 11.8, respectively.

value of CMS result and satisfy the bounds from Higgs data simultaneously, one needs $\chi^\ell_{23} > 5$. That is, with the severe limits of $\tan\beta$ and $c_{\beta\alpha}$, an accurate measurement of $h \to \mu\tau$ could directly bound on $\chi^\ell_{23}$. To clearly show the correlation between $BR(h \to \mu\tau)$ and the parameters constrained by Higgs data, we plot the $BR(h \to \mu\tau)$ in terms of the results of Fig. 3 in Fig. 5(b), where we fix $\chi^\ell_{23} = 5$ and (blue, green, red) stands for the best fit at (68%, 95%, 99.7%) CL.

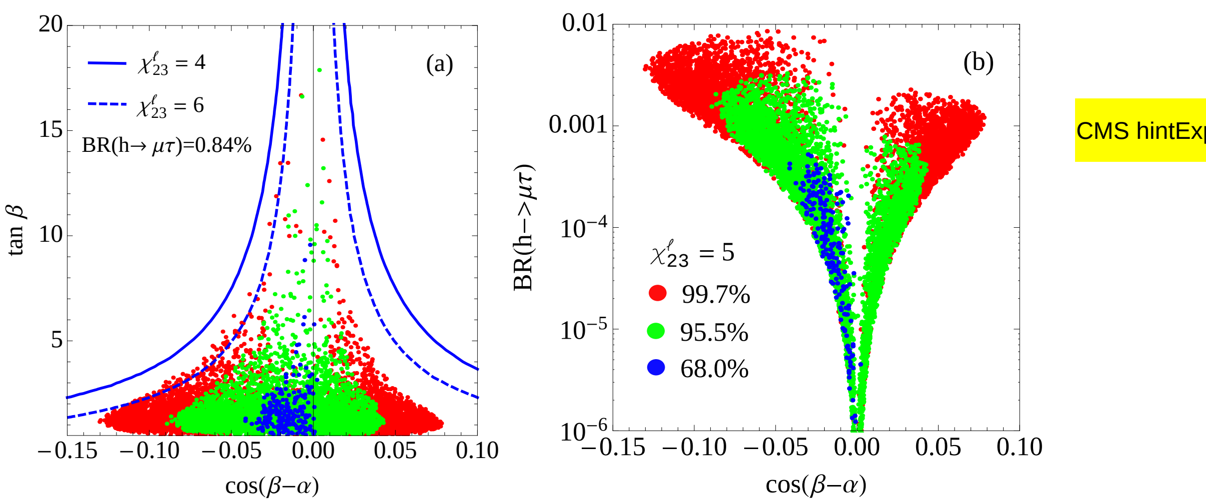


FIG. 5: (a) Contour for $BR(h \to \mu\tau) = 0.84\%$ as a function of $\cos(\beta - \alpha)$ and $\tan\beta$ with $\chi^\ell_{23} = 4$ (solid) and 6 (dashed). (b) $BR(h \to \mu\tau)$ as a function of $\cos(\beta - \alpha)$, where (blue, green, red) stands for the best fit at (68%, 95%, 99.7%) CL.

By Eq. (13), we see that tree-level $\tau \to 3\mu$ decay is sensitive to the masses of $m_{H,A}$, $\tan\beta$ and $\chi^\ell_{23,22}$, but insensitive to $c_{\beta\alpha}$. In Fig. 6(a), we show the contours for $BR(\tau \to 3\mu) \times 10^8$ as a function of $\tan\beta$ and $m_H$, where $m_A = 300$ GeV, $\chi^\ell_{23} = 5$, $\chi^\ell_{22} = -2$ and $c_{\beta\alpha} = -0.05$ are used. The values in the plot denote the BR for $\tau \to 3\mu$ and the largest one is the current upper limit. Although a vanished $\chi^\ell_{22}$ still leads to a sizeable $BR(\tau \to 3\mu)$, however, its value indeed influences the BR for $\tau \to 3\mu$ decay. To understand the effect of $\chi^\ell_{22}$, we plot $BR(\tau \to 3\mu) \times 10^8$ as a function of $\chi^\ell_{23}$ and $\chi^\ell_{22}$ in Fig. 6(b), where we have taken $\tan\beta = 6$ and $m_{H(A)} = 200(300)$ GeV and these values of parameters are consistent with the constraints from Higgs data.

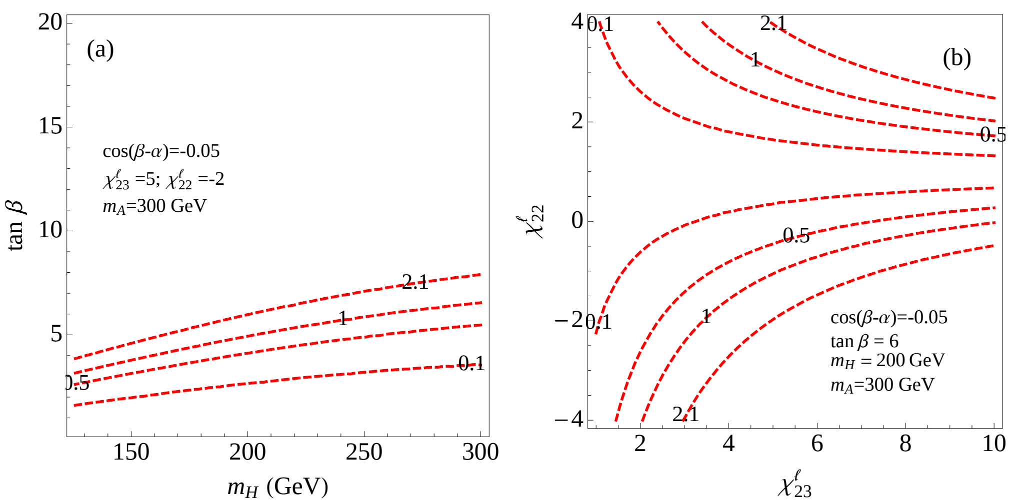


FIG. 6: Contours for $BR(\tau \to 3\mu) \times 10^8$ as a function of (a) $m_H$ and $\tan\beta$ with $\chi^\ell_{23(22)} = 5(-2)$ and (b) $\chi^\ell_{23}$ and $\chi^\ell_{22}$ with $m_H = 200$ GeV and $\tan\beta = 6$. In both plots, $m_A = 300$ GeV and $\cos(\beta - \alpha) = -0.05$ are taken.

By Eq. (A5), we see that besides the parameters $\tan\beta$, $m_{H,A}$ and $\chi^\ell_{23}$, $\tau \to \mu\gamma$ at one-loop level is also dictated by $\chi^\ell_{33}$. Since $c_{\beta\alpha}$ has been limited to a narrow region, like $\tau \to 3\mu$ decay, $\tau \to \mu\gamma$ is insensitive to $c_{\beta\alpha}$. We present the contours for $BR(\tau \to \mu\gamma) \times 10^8$ as a function of $\tan\beta$ and $m_H$ in Fig. 7(a), where we have included one-loop and two-loop contributions and fixed $c_{\beta\alpha} = -0.05$, $\chi^\ell_{23(33)} = 5(0)$ and $m_A = 300$ GeV. The largest value on the curves is the current experimental upper limit. We see that with strict constraints of Higgs data, $BR(\tau \to \mu\gamma)$ in type-III THDM could still be compatible with current upper limit while the decay $h \to \mu\tau$ matches with CMS's observation.

According to Eq. (15), we know that muon $g - 2$ strongly depends on $\chi^\ell_{23}$, $\tan\beta$ and

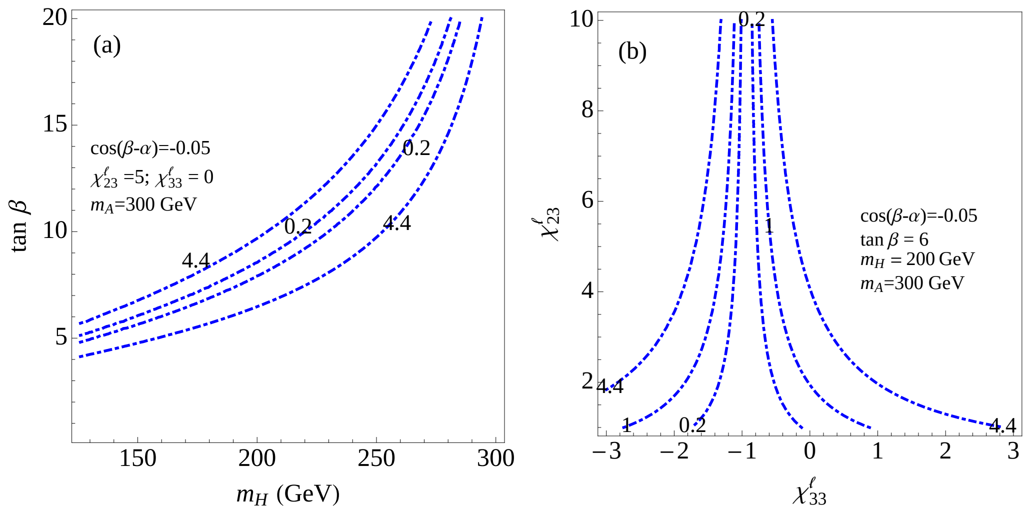


FIG. 7: Contours for $BR(\tau \to \mu\gamma) \times 10^8$ as a function of (a) $\tan\beta$ and $m_H$ with $\chi^\ell_{23}(\chi^\ell_{33}) = 5(0)$ and (b) $\chi^\ell_{23}$ and $\chi^\ell_{33}$ with $\tan\beta = 6$ and $m_{H(A)} = 200(300)$ GeV. One and two loop effects are included.

$m_{H,A}$. It is interesting to see if $\Delta a_\mu$ could be explained in type-III model when the severe bounds of involving parameters are imposed. With $m_A = 300$ GeV, $\chi^\ell_{23} = 5$, we plot the contours for $\Delta a_\mu \times 10^9$ as a function of $\tan\beta$ and $m_H$ in Fig. 8(a), where the shaded region (yellow) stands for the central value with $2\sigma$ errors. By the plot, it is clear that those values of parameters satisfied the Higgs data and $BR(h \to \mu\tau) = 0.84\%$ could also make the $(g-2)_\mu$ consistent with the discrepancy between experiment and SM prediction. Based on Eq. (19), we find that $\mu \to e\gamma$ could be expressed in terms of $\Delta a_\mu$. With the ansatz $X^\ell_{ij} = \sqrt{m_i m_j}/v\chi^\ell_{ij}$, we show the contours for $BR(\mu \to e\gamma)$ as a function of $\Delta a_\mu$ and $\chi^\ell_{13}/\chi^\ell_{23}$ in Fig. 8(b), where the numbers on the curves are the BR for $\mu \to e\gamma$ decay by multiplying a scale of $10^{13}$. Clearly, in order to satisfy the bound from rare $\mu \to e\gamma$ decay, $\chi^\ell_{13}$ has to be less than $\mathcal{O}(10^{-3})$. As a result, we get

$$BR(h \to e\tau) < 2 \times 10^{-4} \left(\frac{\chi^\ell_{13}/\chi^\ell_{23}}{10^{-3}}\right)^2 BR(h \to \mu\tau). \tag{27}$$

Hence, in type-III THDM, $h \to e\tau$ at least is an order of $10^4$ smaller than $h \to \mu\tau$.

Finally, we discuss the decay $Z \to \mu\tau$. Similar to rare $\tau$ decays, in type-III model, $BR(Z \to \mu\tau)$ is sensitive to $\tan\beta$, $m_{H,A}$ and $\chi^\ell_{23(33)}$. Although we do not explicitly show the formulas in the paper, instead we directly present the contours for $BR(Z \to \mu\tau) \times 10^7$ as a function of $\tan\beta$ and $m_H$ in Fig. 9(a), where $m_A = 300$ GeV, $\chi^\ell_{23(33)} = 5(0)$ and $c_{\beta\alpha} = -0.05$

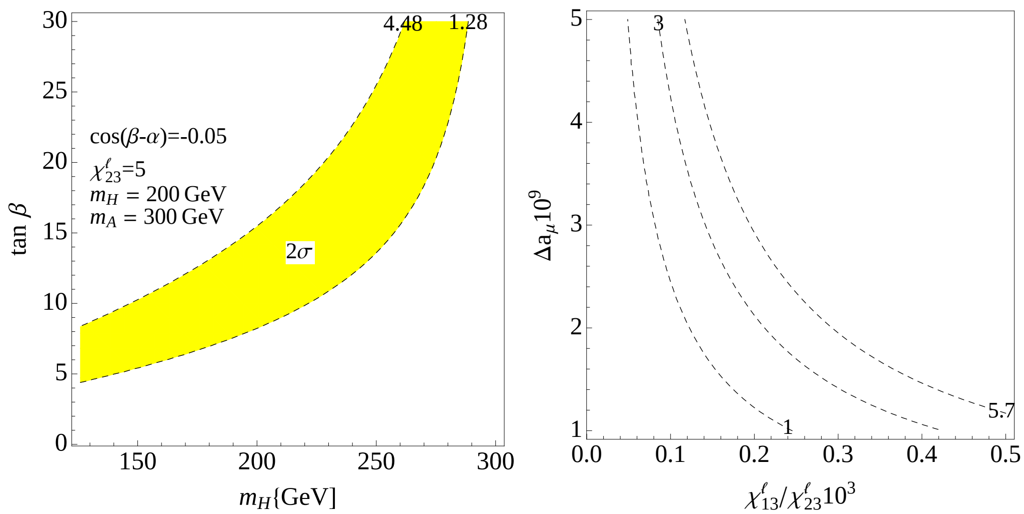


FIG. 8: (a) Contours for $\Delta a_\mu \times 10^9$ as a function of $\tan\beta$ and $m_H$ with $m_A = 300$ GeV, $\chi^\ell_{23} = 5$ and $\cos(\beta - \alpha) = -0.05$ and (b) Contours for $BR(\mu \to e\gamma) \times 10^{13}$ as a function of $\Delta a_\mu$ and $\chi^\ell_{13}/\chi^\ell_{23}$, where the relation in Eq. (19) is adopted.

are used. With the constrained parameters that fit the CMS result of $h \to \mu\tau$, we find that BR for $Z \to \mu\tau$ decay is $BR(Z \to \mu\tau) < 10^{-6}$. The current experimental upper limit is $BR(Z \to \mu\tau)^{\rm exp} < 2.1 \times 10^{-5}$. To understand the dependence of $\chi^\ell_{23}$, we also show the contours as a function of $\tan\beta$ and $\chi^\ell_{23}$ with $m_H = 200$ GeV in Fig. 9(b).

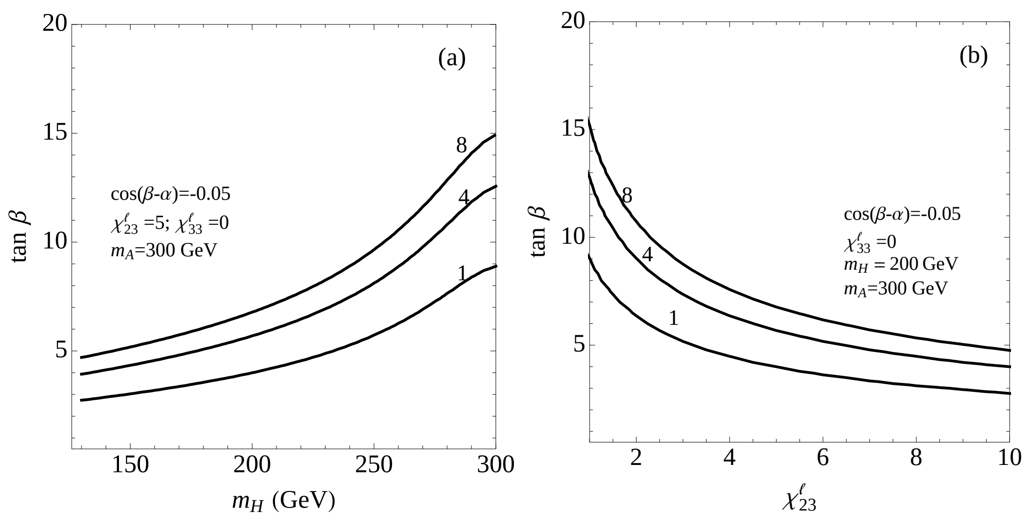


FIG. 9: Contours for $BR(Z \to \mu\tau) \times 10^7$ as a function of (a) $\tan\beta$ and $m_H$ with $\chi^\ell_{23} = 5$ and (b) $\tan\beta$ and $\chi^\ell_{23}$ with $m_H = 200$ GeV. In both plot, we adopt $m_A = 300$ GeV, $\chi^\ell_{33} = 0$ and $\cos(\beta - \alpha) = -0.05$.

In summary, we have revisited the constraints for two-Higgs-doublet model. The bounds from theoretical requirements, precision $\delta\rho$ and oblique-parameter measurements are shown in Fig. 2 and the bounds from Higgs data with $\chi$-square fit at 68%, 95.5% and 99.7% CL are given in Fig. 3. We clearly manifest the tension of Higgs data on the free parameters of new physics. With the values of parameters which are constrained by Higgs data, we find that type-III THDM could fit the CMS result $BR(h \to \mu\tau) = (0.84^{+0.39}_{-0.37})\%$. With the same set of parameters, the resultant branching ratios of tree-level $\tau \to 3\mu$ and loop induced $\tau \to \mu\gamma$ could be consistent with the current experimental upper limits. Under the strict limits of Higgs data, we clearly show that the anomaly of muon anomalous magnetic moment could be explained by type-III model. The rare decay $\mu \to e\gamma$ could be satisfied by small parameter $\chi^{\ell}_{13}$. As a result, we expect that the branching ratio for $h \to e\tau$ is smaller than the decay $h \to \mu\tau$ by $10^4$ in order of magnitude. Additionally, we also calculate the branching ratio for rare decay $Z \to \mu\tau$ and the result is one order of magnitude smaller than current experimental upper limit.


**Acknowledgments**

The work of CHC is supported by the Ministry of Science and Technology of R.O.C. under Grant #: MOST-103-2112-M-006-004-MY3. The work of RB was supported by the Moroccan Ministry of Higher Education and Scientific Research MESRSFC and CNRST: "Projet dans les domaines prioritaires de la recherche scientifique et du développement technologique": PPR/2015/6.


## Appendix A

### 1. Yukawa couplings

The Higgs Yukawa couplings to fermions are given by

$$
\begin{aligned}
-\mathcal{L}^h_Y &= \bar{u}_L\left[\frac{c_\alpha}{v s_\beta}\mathbf{m_u} - \frac{c_{\beta\alpha}}{s_\beta}\mathbf{X}^u\right]u_R h + \bar{d}_L\left[-\frac{s_\alpha}{v c_\beta}\mathbf{m_d} + \frac{c_{\beta\alpha}}{c_\beta}\mathbf{X}^d\right]d_R h \\
&+ \bar{\ell}_L\left[-\frac{s_\alpha}{v c_\beta}\mathbf{m}_\ell + \frac{c_{\beta\alpha}}{c_\beta}\mathbf{X}^\ell\right]\ell_R h + h.c.\,, \qquad \text{(A1)}
\end{aligned}
$$

where $c_{\beta\alpha} = \cos(\beta - \alpha)$, $s_{\beta\alpha} = \sin(\beta - \alpha)$ and $\mathbf{X}^f s$ are defined in Eq. (9). Similarly, the Yukawa couplings of scalars $H$ and $A$ are expressed by

$$\begin{aligned}
-\mathcal{L}_Y^{H,A} &= \bar{u}_L \left[ \frac{s_\alpha}{v s_\beta} \mathbf{m_u} + \frac{s_{\beta\alpha}}{s_\beta} \mathbf{X}^u \right] u_R H + \bar{d}_L \left[ \frac{c_\alpha}{v c_\beta} \mathbf{m_d} - \frac{s_{\beta\alpha}}{c_\beta} \mathbf{X}^d \right] d_R H \\
&+ \bar{\ell}_L \left[ \frac{c_\alpha}{v c_\beta} \mathbf{m}_\ell - \frac{s_{\beta\alpha}}{c_\beta} \mathbf{X}^\ell \right] \ell_R H + i\bar{u}_L \left[ -\frac{\cot\beta}{v} \mathbf{m_u} + \frac{\mathbf{X}^u}{s_\beta} \right] u_R A \\
&+ i\bar{d}_L \left[ -\frac{\tan\beta}{v} \mathbf{m_d} + \frac{\mathbf{X}^d}{c_\beta} \right] d_R A + i\bar{\ell}_L \left[ -\frac{\tan\beta}{v} \mathbf{m}_\ell + \frac{\mathbf{X}^\ell}{c_\beta} \right] \ell_R A + h.c. \qquad \text{(A2)}
\end{aligned}$$

The Yukawa couplings of charged Higgs to fermions are

$$\begin{aligned}
-\mathcal{L}_Y^{H^\pm} &= \sqrt{2}\bar{u}_L V_{CKM}^\dagger \left[ -\frac{\cot\beta}{v} \mathbf{m_u} + \frac{\mathbf{X}^u}{s_\beta} \right] d_R H^- \\
&+ \sqrt{2}\bar{d}_L V_{\text{CKM}} \left[ -\frac{\tan\beta}{v} \mathbf{m_d} + \frac{\mathbf{X}^d}{c_\beta} \right] u_R H^+ \\
&+ \sqrt{2}\bar{\nu}_L V_{\text{PMNS}} \left[ -\frac{\tan\beta}{v} \mathbf{m}_\ell + \frac{\mathbf{X}^\ell}{c_\beta} \right] \ell_R H^+ + h.c.\,, \qquad \text{(A3)}
\end{aligned}$$

where CKM and PMNS stand for Cabibbo-Kobayashi-Maskawa and Pontecorvo-Maki-Nakagawa-Sakata matrices, respectively. Except the factor $\sqrt{2}$, CKM and PMNS matrices, the Yukawa couplings of charged Higgs are the same as those of pseudoscalar $A$.

### 2. $\tau \to \mu\gamma$ decay

The effective interaction for $\tau \to \mu\gamma$ is expressed by

$$\mathcal{L}_{\tau\to\mu\gamma} = \frac{e}{16\pi^2} m_\tau \bar{\mu} \sigma_{\mu\nu} \left( C'_L P_L + C'_R P_R \right) \tau F^{\mu\nu}\,, \qquad \text{(A4)}$$

where the Wilson coefficients $C'_L$ and $C'_R$ from one-loop neutral and charged scalars are formulated by

$$\begin{aligned}
C'_{L(R)} &= \sum_{\phi=h,H,A,H^\pm} C'^{\phi}_{L(R)}\,, \\
C'^h_L &= \frac{c_{\beta\alpha} X^\ell_{32}}{2m_h^2 c_\beta} y^\ell_{h33} \left( \ln\frac{m_h^2}{m_\tau^2} - \frac{4}{3} \right)\,, \; C'^H_L = \frac{-s_{\beta\alpha} X^\ell_{32}}{2m_H^2 c_\beta} y^\ell_{H33} \left( \ln\frac{m_H^2}{m_\tau^2} - \frac{4}{3} \right)\,, \\
C'^A_L &= -\frac{X^\ell_{32}}{2m_A^2 c_\beta} y^\ell_{A33} \left( \ln\frac{m_A^2}{m_\tau^2} - \frac{5}{3} \right)\,, \; C'^{H^\pm}_L = -\frac{1}{12 m_{H^\pm}^2} \left( \frac{\sqrt{2} X^\ell_{32}}{c_\beta} \right) y^\ell_{H^\pm 33}\,, \qquad \text{(A5)}
\end{aligned}$$

$C_R^{\prime h,H,A} = C_L^{\prime h,H,A}$ and $C_R^{\prime H^\pm} = 0$. In addition, the contributions from two loops are given by [7, 54, 55]

$$
\begin{aligned}
C_{2L}^{ht(b)} = C_{2R}^{ht(b)} &= 2\frac{c_{\beta\alpha}X_{32}y_{h33}^{u(d)}}{c_\beta}\frac{N_cQ_f^2\alpha}{\pi}\frac{1}{m_\tau m_{t(b)}}f\left(\frac{m_{t(b)}^2}{m_h^2}\right), \\
C_{2L}^{Ht(b)} = C_{2R}^{Ht(b)} &= -2\frac{s_{\beta\alpha}X_{32}y_{H33}^{u(d)}}{c_\beta}\frac{N_cQ_f^2\alpha}{\pi}\frac{1}{m_\tau m_{t(b)}}f\left(\frac{m_{t(b)}^2}{m_H^2}\right), \\
C_{2L}^{At(b)} = C_{2R}^{At(b)} &= -2\frac{X_{32}y_{A33}^{u(d)}}{c_\beta}\frac{N_cQ_f^2\alpha}{\pi}\frac{1}{m_\tau m_{t(b)}}f\left(\frac{m_{t(b)}^2}{m_A^2}\right), \\
C_{2L}^{W} = C_{2R}^{W} &= \frac{s_{\beta\alpha}c_{\beta\alpha}X_{32}}{c_\beta}\frac{g\alpha}{2\pi m_\tau m_W}\Bigg[3f\left(\frac{m_W^2}{m_H^2}\right)+\frac{23}{4}g\left(\frac{m_W^2}{m_H^2}\right)+\frac{3}{4}h\left(\frac{m_W^2}{m_H^2}\right) \\
&\quad +\frac{m_H^2}{2m_W^2}\left(f\left(\frac{m_W^2}{m_H^2}\right)-g\left(\frac{m_W^2}{m_H^2}\right)\right)\Bigg]-(m_H\to m_h)\,,
\end{aligned}
\tag{A6}
$$

where the loop functions are

$$
\begin{aligned}
f(z) &= \frac{z}{2}\int_0^1 dx\frac{(1-2x(1-x))}{x(1-x)-z}\ln\frac{x(1-x)}{z}\,, \\
g(z) &= \frac{z}{2}\int_0^1 dx\frac{1}{x(1-x)-z}\ln\frac{x(1-x)}{z}\,, \\
h(z) &= -\frac{z}{2}\int_0^1 dx\frac{1}{x(1-x)-z}\left[1-\frac{z}{x(1-x)-z}\ln\frac{x(1-x)}{z}\right].
\end{aligned}
\tag{A7}
$$

The BR for $\tau\to\mu\gamma$ is expressed by

$$
\frac{BR(\tau\to\mu\gamma)}{BR(\tau\to\mu\bar{\nu}_\mu\nu_\tau)} = \frac{3\alpha_e}{4\pi G_F^2}\left(|C_L'|^2+|C_R'|^2\right). \tag{A8}
$$

---


[1] M. E. Gomez, T. Hahn, S. Heinemeyer and M. Rehman, Lepton-Flavor-Violating MSSM," Phys. Rev. D **90**, no. 7, 074016 (2014) [arXiv:1408.0663 [hep-ph]].

[2] G. Aad *et al.* [ATLAS Collaboration], "Observation of a new particle in the search for the Standard Model Higgs boson with the ATLAS detector at the LHC", Phys. Lett. B **716**, 1 (2012) [arXiv:1207.7214 [hep-ex]].

[3] S. Chatrchyan *et al.* [CMS Collaboration], "Observation of a new boson at a mass of 125 GeV with the CMS experiment at the LHC", Phys. Lett. B **716**, 30 (2012) [arXiv:1207.7235 [hep-ex]].

[4] V. Khachatryan *et al.* [CMS Collaboration], Phys. Lett. B **749**, 337 (2015) [arXiv:1502.07400 [hep-ex]].

[5] G. Aad *et al.* [ATLAS Collaboration], arXiv:1508.03372 [hep-ex].

[6] M. D. Campos, A. E. C. Hernandez, H. Pas and E. Schumacher, Phys. Rev. D **91**, no. 11, 116011 (2015) [arXiv:1408.1652 [hep-ph]].

[7] D. Aristizabal Sierra and A. Vicente, Phys. Rev. D **90**, no. 11, 115004 (2014) [arXiv:1409.7690 [hep-ph]].

[8] C. J. Lee and J. Tandean, JHEP **1504**, 174 (2015) [arXiv:1410.6803 [hep-ph]].

[9] J. Heeck, M. Holthausen, W. Rodejohann and Y. Shimizu, Nucl. Phys. B **896**, 281 (2015) [arXiv:1412.3671 [hep-ph]].

[10] A. Crivellin, G. DAmbrosio and J. Heeck, Phys. Rev. Lett. **114**, 151801 (2015) [arXiv:1501.00993 [hep-ph]].

[11] I. Dorsner, S. Fajfer, A. Greljo, J. F. Kamenik, N. Kosnik and I. Nisandzic, JHEP **1506**, 108 (2015) [arXiv:1502.07784 [hep-ph]].

[12] Y. Omura, E. Senaha and K. Tobe, JHEP **1505**, 028 (2015) [arXiv:1502.07824 [hep-ph]].

[13] A. Crivellin, G. DAmbrosio and J. Heeck, Phys. Rev. D **91**, no. 7, 075006 (2015) [arXiv:1503.03477 [hep-ph]].

[14] D. Das and A. Kundu, Phys. Rev. D **92**, no. 1, 015009 (2015) [arXiv:1504.01125 [hep-ph]].

[15] F. Bishara, J. Brod, P. Uttayarat and J. Zupan, arXiv:1504.04022 [hep-ph].

[16] X. G. He, J. Tandean and Y. J. Zheng, JHEP **1509**, 093 (2015) doi:10.1007/JHEP09(2015)093 [arXiv:1507.02673 [hep-ph]].

[17] C. W. Chiang, H. Fukuda, M. Takeuchi and T. T. Yanagida, JHEP **1511**, 057 (2015) [arXiv:1507.04354 [hep-ph]].

[18] W. Altmannshofer, S. Gori, A. L. Kagan, L. Silvestrini and J. Zupan, arXiv:1507.07927 [hep-ph].

[19] K. Cheung, W. Y. Keung and P. Y. Tseng, arXiv:1508.01897 [hep-ph].

[20] E. Arganda, M. J. Herrero, X. Marcano and C. Weiland, arXiv:1508.04623 [hep-ph].

[21] F. J. Botella, G. C. Branco, M. Nebot and M. N. Rebelo, arXiv:1508.05101 [hep-ph].

[22] S. Baek and K. Nishiwaki, arXiv:1509.07410 [hep-ph].

[23] W. Huang and Y. L. Tang, Phys. Rev. D **92**, 094015 (2015) [arXiv:1509.08599 [hep-ph]].

[24] S. Baek and Z. F. Kang, arXiv:1510.00100 [hep-ph].

[25] E. Arganda, M. J. Herrero, R. Morales and A. Szynkman, arXiv:1510.04685 [hep-ph].

[26] D. Aloni, Y. Nir and E. Stamou, arXiv:1511.00979 [hep-ph].

[27] G. Blankenburg, J. Ellis and G. Isidori, Phys. Lett. B **712**, 386 (2012) [arXiv:1202.5704 [hep-ph]].

[28] A. Arhrib, Y. Cheng and O. C. W. Kong, Europhys. Lett. **101**, 31003 (2013) [arXiv:1208.4669 [hep-ph]].

[29] R. Harnik, J. Kopp and J. Zupan, JHEP **1303**, 026 (2013) [arXiv:1209.1397 [hep-ph]].

[30] A. Dery, A. Efrati, Y. Hochberg and Y. Nir, JHEP **1305**, 039 (2013) [arXiv:1302.3229 [hep-ph]].

[31] M. Arroyo, J. L. Diaz-Cruz, E. Diaz and J. A. Orduz-Ducuara, arXiv:1306.2343 [hep-ph].

[32] A. Celis, V. Cirigliano and E. Passemar, Phys. Rev. D **89**, 013008 (2014) [arXiv:1309.3564 [hep-ph]].

[33] A. Falkowski, D. M. Straub and A. Vicente, JHEP **1405**, 092 (2014) [arXiv:1312.5329 [hep-ph]].

[34] A. Dery, A. Efrati, Y. Nir, Y. Soreq and V. Susic, Phys. Rev. D **90**, 115022 (2014) [arXiv:1408.1371 [hep-ph]].

[35] T. D. Lee, Phys. Rev. D **8**, 1226 (1973); T. D. Lee, Phys. Rept. **9**, 143 (1974).

[36] G. C. Branco, P. M. Ferreira, L. Lavoura, M. N. Rebelo, M. Sher and J. P. Silva, Phys. Rept. **516**, 1 (2012) [arXiv:1106.0034 [hep-ph]].

[37] K.A. Olive et al. (Particle Data Group), Chin. Phys. C, 38, 090001 (2014).

[38] K. A. Assamagan, A. Deandrea and P. A. Delsart, Phys. Rev. D **67**, 035001 (2003) [hep-ph/0207302].

[39] S. Davidson and G. J. Grenier, Phys. Rev. D **81**, 095016 (2010) [arXiv:1001.0434 [hep-ph]].

[40] A. Masiero and T. Yanagida, hep-ph/9812225.

[41] K. S. Babu, B. Dutta and R. N. Mohapatra, Phys. Rev. D **61**, 091701 (2000) [hep-ph/9905464].

[42] J. F. Gunion, H. E. Haber, G. L. Kane and S. Dawson, Front. Phys. **80**, 1 (2000).

[43] T. Hahn and M. Perez-Victoria, Comput. Phys. Commun. **118**, 153 (1999) [hep-ph/9807565].

[44] A. G. Akeroyd, A. Arhrib and E. M. Naimi, Phys. Lett. B **490**, 119 (2000) [hep-ph/0006035].

[45] M. Sher, Phys. Rept. **179**, 273 (1989).

[46] P. M. Ferreira, R. Santos and A. Barroso, Phys. Lett. B **603**, 219 (2004) [hep-ph/0406231]; Phys. Lett. B **629**, 114 (2005). .

[47] M. E. Peskin and T. Takeuchi, Phys. Rev. D **46**, 381 (1992).

[48] M. Baak *et al.* [Gfitter Group Collaboration], Eur. Phys. J. C **74** (2014) 3046 [arXiv:1407.3792 [hep-ph]].

[49] J. F. Gunion and H. E. Haber, Phys. Rev. D **67**, 075019 (2003) [hep-ph/0207010].

[50] M. Misiak *et al.*, Phys. Rev. Lett. **114**, 221801 (2015) [arXiv:1503.01789 [hep-ph]].

[51] ATALS Collaboration, ATLAS-CONF-2013-034.

[52] CMS Collaboration, CMS-PAS-HIG-13-005.

[53] A. Arhrib, R. Benbrik, C. H. Chen, M. Gomez-Bock and S. Semlali, arXiv:1508.06490 [hep-ph].

[54] D. Chang, W. S. Hou and W. Y. Keung, Phys. Rev. D **48**, 217 (1993) [hep-ph/9302267].

[55] S. Davidson and G. J. Grenier, Phys. Rev. D **81**, 095016 (2010) [arXiv:1001.0434 [hep-ph]].